Methods 94 (2016) 13–18

Contents lists available at ScienceDirect

Methods

journal homepage: www.elsevier.com/locate/ymeth

# Uncovering mechanosensing mechanisms at the single protein level using magnetic tweezers

Shimin Le [a,b,c], Ruchuan Liu [b,d], Chwee Teck Lim [a,e,f,*], Jie Yan [a,b,c,*]

[a] Mechanobiology Institute, National University of Singapore, Singapore 117411, Singapore
[b] Department of Physics, National University of Singapore, Singapore 117542, Singapore
[c] Centre for Bioimaging Sciences, National University of Singapore, Singapore 117546, Singapore
[d] College of Physics, Chongqing University, Chongqing 401331, China
[e] Department of Biomedical Engineering, National University of Singapore, Singapore 117575, Singapore
[f] Department of Mechanical Engineering, National University of Singapore, Singapore 117575, Singapore

ARTICLE INFO

*Article history:*
Received 29 April 2015
Received in revised form 1 August 2015
Accepted 25 August 2015
Available online 28 August 2015

*Keywords:*
Single-molecule magnetic tweezers
Mechanosensing proteins
Vinculin
Talin
α-Catenin
Titin immunoglobulin domain

ABSTRACT

Mechanosensing of the micro-environments has been shown to be essential for cell survival, growth, differentiation and migration. The mechanosensing pathways are mediated by a set of mechanosensitive proteins located at focal adhesion and cell–cell adherens junctions as well as in the cytoskeleton network. Here we review the applications of magnetic tweezers on elucidating the molecular mechanisms of the mechanosensing proteins. The scope of this review includes the principles of the magnetic tweezers technology, theoretical analysis of force-dependent stability and interaction of mechanosensing proteins, and recent findings obtained using magnetic tweezers.



## 1. Introduction

In tissues, cells need to adapt to their microenvironment by sensing various chemical and physical cues. Recent development in cell biology has demonstrated mechanical force as one of the critical determinants involved in cell migration, cell differentiation, tissue development and maintenance. In tissues, cells adhere to extracellular matrix (ECM) through formation of integrin dependent focal adhesion and to the neighboring cells through cadherin dependent cell–cell adherens junctions. Forces are generated by actomyosin contraction, and propagated in the whole tissue [1,2]. Force sensing of cells is mediated by a set of mechanosensing proteins located at focal adhesion and cell–cell adherens junctions as well as in the cytoskeleton network (Fig. 1). It has been proposed that such mechanosensing proteins can change their conformations under force, resulting in switching their binding partners in a force-dependent manner. This way, they can process the mechanical cues into downstream biochemical reactions, resulting in mechanosensing signaling of cells [2].

In spite of the simplicity of the above hypothesis of the mechanosensing mechanism, it is technically challenging to directly test it in experiments. In order to do so, well-controlled forces in the physiological level (pN range) have to be applied to individual proteins, and the resulting dynamic conformational change of the proteins has to be probed at a nanometer resolution. In addition, the force-dependent interactions of the force-bearing mechanosensing proteins with their binding partners need to be investigated at a single-molecule level in real time. Thanks to the rapidly developing single-molecule manipulation technologies, such as atomic force spectroscopy (often referred as AFM, short for atomic force microscopy), optical tweezers, and magnetic tweezers [3], probing force-dependent conformational changes and interactions quantitatively at a single-molecule level has become possible. In addition to *in vitro* single-molecule manipulation experiments, Föster Resonance Energy Transfer (FRET) based force sensor has also been developed to measure force applied to mechanosensitive proteins *in vivo* [4,5].

However, applications of the single-molecule manipulation technologies to the studies of mechanosensing proteins are still challenging due to various technical limitations of the respective

* Corresponding authors at: Department of Biomedical Engineering and Mechanobiology Institute, National University of Singapore, Singapore 117575, Singapore (C.T. Lim), Department of Physics and Mechanobiology Institute, National University of Singapore, Singapore 117411, Singapore (J. Yan).
*E-mail addresses:* ctlim@nus.edu.sg (C.T. Lim), phyyj@nus.edu.sg (J. Yan).

http://dx.doi.org/10.1016/j.ymeth.2015.08.020
1046-2023/

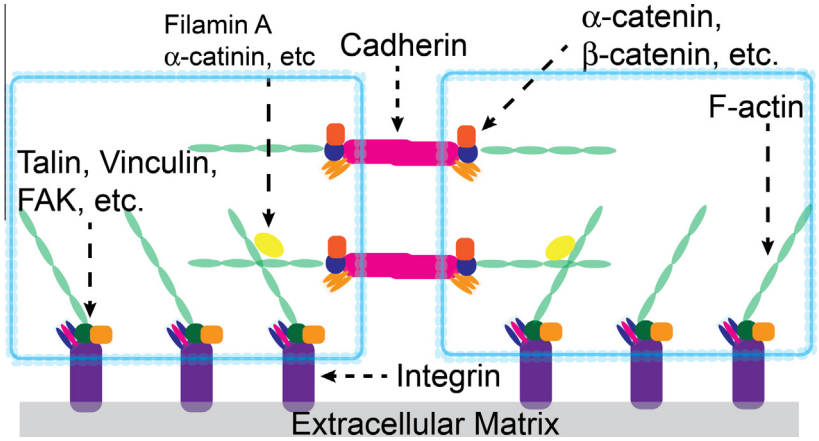


**Fig. 1.** Schematics of integrin mediated cell-matrix and cadherin mediated cell–cell adhesions. Actin cytoskeleton network and several known mechanosensitive proteins are highlighted.

technologies to apply low forces (pN range) directly to short tethers (<100 nm) over long duration of experiments (minutes to hours). One major difficulty is that the experimental time scale needed to study force-dependent conformational changes and interactions of single molecules often exceeds that can be provided by most of current single-molecule manipulation technologies due to rapid mechanical and thermal drifts. For example, the extensively studied 27th titin immunoglobulin (Ig) domain (I27) can be unfolded at a small force of ~5 pN, but with an ultraslow unfolding rate of $\sim 10^{-4}\ s^{-1}$ at this force range [6]. Therefore, studies of such proteins require a very long experimental time scale of several hours at <10 pN forces. Among the three main single-molecule manipulation technologies, magnetic tweezers excel in this aspect by providing the best long-time stability. In the subsequent sections, we review the basic principles of magnetic tweezers, thermodynamics of force sensing, and the recent applications of magnetic tweezers in studies of the molecular mechanisms of mechanosensing proteins.

## 2. Principles of magnetic tweezers

### 2.1. Magnetic tweezers apparatus

The basic idea of magnetic tweezers is to use an external magnetic field to apply forces to a paramagnetic bead typical with a diameter of 1–3 μm. When the bead is tethered to an end of a molecule with the other end of the molecule attached to a fixed surface, the molecule is then subject to an external force. In 1998, a highly efficient design of magnetic tweezers that is suitable for high resolution single-molecule studies was published by Strick et al. [7]. In this design, a basic magnetic tweezers apparatus consists of a reaction channel mounted on a microscope stage in which single-molecule tethers are formed, an optical microscope to image the tethered bead, a camera to record the bead images, permanent or electric magnets to generate a force perpendicular to the focal plane ($x$–$y$ plane), and a computer to control the tweezers and analyze the bead fluctuation to obtain essential information of force and extension change of molecule (schematics in Fig. 2A). In this vertical design, the extension change is based on analyzing the diffraction patterns of the bead at different heights from the surface, which has been adopted by many other labs. Besides the perpendicular design, a transverse design was also developed, which applies forces in the focal plane. In the transverse design, the extension is determined by the centroid of bead [8].

The two designs have their respective strengths. In the vertical design, the tethers are formed on large coverslip surface, suitable for high-throughput multiplexing experiments [9,10]. The length of tethers can be shorter than 200 nm, ideal for high signal-to-noise measurements [11–14]. The tweezers can be built on a total internal reflection fluorescence microscope [15], allowing combination with single-molecule spectroscopy technologies such as single-molecule FRET (smFRET) [16,17]. In the transverse design, tethers can be as long as the dimension of the whole view area, ideal for studies of large DNA condensation by proteins [18–20]. The tethers are stretched in the focal plane, allowing direct observation of fluorescence labeled proteins on DNA [20]. The position of the bead can be determined with nanometer accuracy with long working distance non-contact objective, making it possible to control the temperature of the sample independently from the microscope, convenient for temperature dependent studies [21–23]. In the subsequent sections, we focus on the vertical design of the magnetic tweezers because of its strength in directly stretching short tethers formed by mechanosensing proteins.

### 2.2. Force generation

*Force generation.* As illustrated in Fig. 2B, a pair of magnets is placed above the sample stage, with its geometric center aligned along the optical axis. It produces a magnetic field, $\vec{B}$, along $\hat{x}$-direction (Fig. 1A and B) and a gradient perpendicular towards the magnets ($\hat{z}$-direction). The resulting force, $\vec{F} = \bigtriangledown(\vec{M}\cdot\vec{B}) = \hat{z}\frac{d}{dz}(\vec{M}\cdot\vec{B})$, where $\vec{M}$ is the induced magnet moment of the bead, is therefore along the $\hat{z}$-direction. In typical magnetic tweezers setup, the magnetization of the bead is saturated, resulting in a constant magnitude of $M_{max}$. Hence, the bead experiences a force, $\vec{F} = \hat{z}M_{max}B'(z)$. The logarithm of the magnitude of force, $\ln F = \ln M_{max} + \ln B'(z)$, consists of two independent contributions from the properties of bead and the magnets, respectively. For a given magnet-bead distance ($d$), forces applied to two different beads differ only by a constant $\Delta \ln F_{1,2}(d) = \Delta \ln M_{max,\,1,2} = \delta_{1,2}$. The slope $F'(d)$ is $< 10^{-2}$ pN/μm for typical magnetic tweezers settings [3,11,6]. Therefore, force is insensitive to drift in $d$ and can remain stable over long time scale (hours). Furthermore, the spatial drift of the 3D position of the tethered bead can be effectively eliminated when a stuck bead is used as a reference [11,6]. The magnitude of the force can be tuned by controlling $d$. Various force controls, such as constant force (constant $d$) and loading-rate control with linearly increasing force (by programmed $d(t)$), can be easily achieved by moving the magnets using a computer-controlled motorized manipulator.

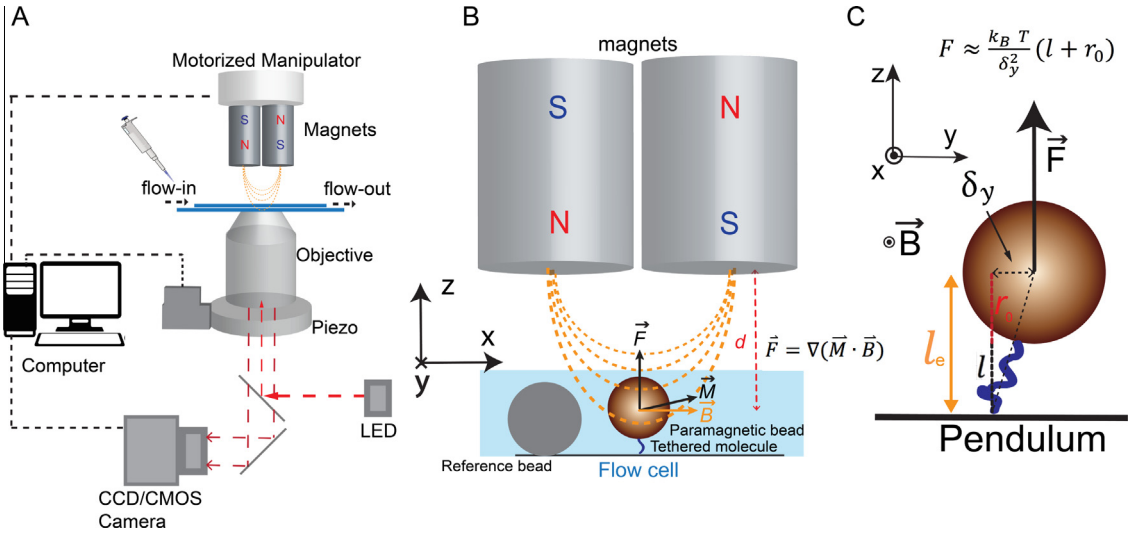


**Fig. 2.** Magnetic tweezers setup. (A) Basic apparatus that includes a piezo controlled objective, a camera to record bead images, a flow chamber in which protein tethers are formed, a pair of magnets above the chamber that generates force, and a computer controlling system. (B) Directions of the magnetic field $\vec{B}$, magnetization of bead $\vec{M}$, and force $\vec{F}$. Note that $\vec{M}$ is often tilted from $\vec{B}$ due to the heterogeneity of the magnetization of the bead and the off-center tethering of the molecule [11,6]. (C) Force calibration based on the bead fluctuation along the direction perpendicular to $\vec{B}$ and $\vec{F}$.

### 2.3. Force calibration

In principle, the force applied to a tether can be obtained by analyzing the thermal motion of the bead in the $x$–$y$ plane, which is considered as a pendulum motion with an effective length $l_e$ through $F \sim \frac{k_B T}{\delta^2} l_e$ (Fig. 2C). Here $\delta^2$ is the variance of bead fluctuation along a direction. In the magnets geometry shown in Fig. 2A, due to the alignment of the anisotropic magnetization axis of bead along the magnetic field direction (i.e., $\hat{x}$), the bead displacement in $\hat{x}$ is dominated by the fluctuation of the molecule, while that in $\hat{y}$ has an additional contribution from bead rotation around the attaching point to the molecule [11]. Therefore, the effective length of pendulum $l_e$, is approximately the extension $z$ of the molecule if using the motion in the $\hat{x}$-direction and $z + r$ if using the motion in the $\hat{y}$-direction, where $r$ is the radius of the bead.

To accurately determine the equilibrium fluctuation of the bead position, the sampling rate $f_s$ has to be faster than the Lorentzian corner frequency, $f_c = \frac{F}{2\pi\gamma l_e}$, where $\gamma = 6\pi\eta r$ is the drag coefficient of the bead and $\eta$ is the viscosity of the solution medium. In typical magnetic tweezers experiments, beads with $r \sim 0.5 - 3$ μm are used. A CCD or CMOS camera is used to acquire bead images with $f_s \sim 100$ Hz. Using the commonly used 2.8-μm-diameter dynalbead M-280 bead (invitrogen) for example, this method can obtain forces up to $\sim 100$ pN for $l_e = 10$ μm, while less than 1 pN for $l_e < 100$ nm. In single-protein manipulation studies, $z$ is typically <100 nm; therefore, the above force calibration method can calibrate <1 pN force using $\hat{x}$-fluctuation. However, it can be expanded to ~15 pN using $\hat{y}$-fluctuation due to the increased effective pendulum length $l_e = z + r$ [11].

Forces >15 pN can be obtained by an extrapolation method, by utilizing the property that $\Delta \ln F_{1,2}(d) = \Delta \ln M_{\max,1,2} = \delta_{1,2}$ between two different beads [11]. The extrapolation is based on a standard curve, $F^*(d)$, that is calibrated using long DNA (48,502 bp, $\lambda$-DNA) molecules up to 100 pN. In single-protein manipulation experiments, forces at < 15 pN are directly calibrated based on the bead fluctuation along the $\hat{y}$ direction, which also determined the shift $\delta_{1,2}$. With the determined shift, forces at >15 pN can be obtained by extrapolation using the standard curve through the relation: $\ln F(d) = \ln F^*(d) + \delta_{1,2}$. Using this method, forces up to 100 pN can be determined with a relative error of around 10%, which is mainly caused by the uncertainty in the radius of the commercially available beads [11].

## 3. Force-dependent stability and interactions

In order to apply magnetic tweezers to investigate the molecular mechanisms of mechanosensing proteins, one has to understand their force-dependent stability and interactions. A folded protein domain can be considered as a rigid body. Force tends to align the straight line connecting the two force-attaching points along the force direction in competition with thermal fluctuation. This results in a simple force-extension curve (which is a monomeric freely-joint chain force-extension curve) [24–26,6]:

$$\frac{z_{\text{folded}}}{l_0} = \left(\coth\left(\frac{Fl_0}{k_B T}\right) - \frac{k_B T}{Fl_0}\right), \tag{1}$$

where $l_0$ is the length between the two force-attaching point, $k_B$ is the Boltzmann constant and $T$ is the absolute temperature.

The force-extension curve of an unfolded protein is contributed by the flexible polypeptide chain, which can be described by the worm-like chain (WLC) model through the Marko–Siggia formula [27,28] with a small bending persistence of $A \approx 0.6 - 0.8$ nm [6]:

$$\frac{FA}{k_B T} = \frac{1}{4(1 - z_{\text{unfolded}}/L)^2} - \frac{1}{4} + \frac{z_{\text{unfolded}}}{L}, \tag{2}$$

where $L$ is the contour length of unfolded peptide chain.

Under a force constraint of $F$, the energies of the folded and unfolded states are [29,30]:

$$g_1(F) = -\mu_0 + \Phi_1(F), \tag{3a}$$

$$g_2(F) = \Phi_2(F), \tag{3b}$$

where "1" and "2" denote the folded and unfolded states, respectively; $\mu_0$ denotes the resting folding energy of the protein at zero force; $\Phi_i(F)$ $(i = 1 \text{ or } 2)$ denotes the force-dependent conformational energy of the state "$i$", which can be calculated from the corresponding force-extension curve [24–26,6]:

$$\Phi_i(F) = -\int_0^F z_i(f)df. \tag{4}$$

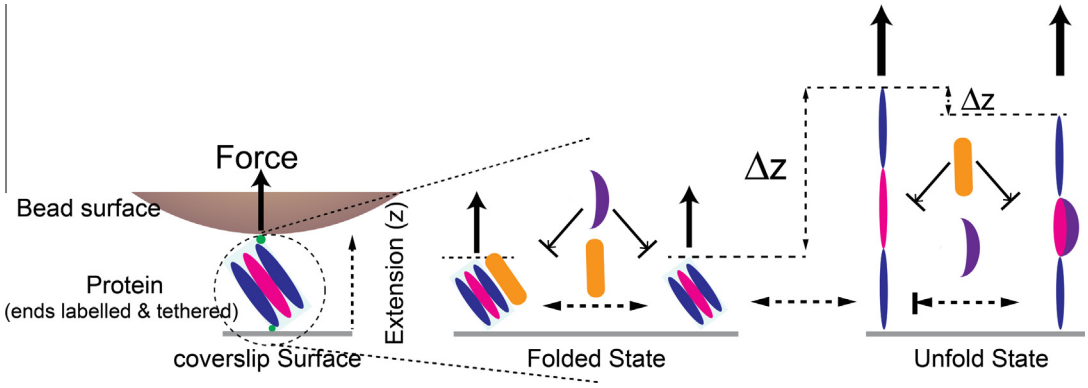


**Fig. 3.** Schematics of applications in studies of force-dependent stability and interactions of mechanosensing proteins. It shows a protein tether that is subject to forces applied by magnetic tweezers. The folded state is a substrate for binding by a cellular factor *A* indicated by the orange bar. In addition, it contains a cryptic binding site for another cellular factor *B* indicated by the purple crescent. The protein is unfolded at increased force, losing the binding interface for *A* while exposing the binding site for *B*. The resulting force-dependent switch of binding partners provides a general mechanism for a variety of mechanosensing processes.

The equilibrium probabilities of the two states are determined by the Boltzmann distributions:

$$P_i(F) = e^{-\beta g_i(F)}/(e^{-\beta g_1(F)} + e^{-\beta g_2(F)}). \quad (5)$$

The critical force $F_c$ at which the two states have equal probabilities is determined by $g_1(F_c) = g_2(F_c)$, i.e.,

$$\Delta\Phi(F_c) = \Phi_2(F_c) - \Phi_1(F_c) = -\mu_0. \quad (6)$$

If $F_c$ is measured, then the resting folding energy is determined. More details of the two-state model can be found in [26].

The above two-state model can be generalized to include more structural states. For example, an α-helix protein domain often consists of several α-helices which are organized as a bundle by hydrophobic interactions. Therefore, three states are needed to describe the conformations of such domains, namely the folded bundling state associated with a bundling energy, a chain of unbundled α-helices associated with a helix formation energy, and completely unfolded peptide chain. The force-dependent probabilities can be obtained similarly by including the contributions of the force-dependent conformational free energies of the respective states. Further, force-dependent interactions can also be treated similarly, by considering the protein bound with a ligand a new state associated with a binding energy of $-k_BT\ln\frac{c}{k_D}$ and a force-dependent conformational energy of the bound state $\Phi_{on}(F)$ [31,26,32,33]. Here $c$ is the concentration of ligands and $k_D$ is the dissociation constant of the binding.

## 4. Recent applications

### *4.1. Dynamics and stability of mechanically stable protein domains under low forces*

The superior capability of long duration of measurements provided by magnetic tweezers makes them ideal tools to study mechanically stable force-bearing protein domains. An example is the immunoglobulin (Ig) domains in the giant titin proteins, which provide the passive elasticity of muscle through unfolding under mechanical stretching during muscle contraction [34]. However, it has been challenging to investigate the mechanical stability of these domains under low force, because of their ultra slow unfolding and refolding transition kinetics. As a result, most previous single-molecule stretching studies of these protein domains using AFM were carried out at high forces (>100 pN) to speed up the unfolding transition. Recently, using ultrastable magnetic tweezers, the force-dependent unfolding and refolding transitions of the I27 domain were studied at low forces (<10 pN) [6].

This is the first time that the mechanical stability and the transition kinetics of the I27 domain were determined under near equilibrium conditions. Applying Eqs. (1–6), the study led to determination of the critical force (~5.4 pN) at which the unfolded and folded states have equal probabilities and a resting folding energy of $\mu_0 \sim 8.3\ k_BT$. At the critical force, the transitions are associated with ultra slow rates of $\sim 10^{-4}\ s^{-1}$, making it challenging to be probed. The result has an important implication that long duration of low force stretching of muscle in activities such as yoga may change the muscle elastic state significantly. This example demonstrates the unique strength of magnetic tweezers in studies of mechanically stable force-bearing Ig domains presenting in many important force-sensing proteins such as titin and filamin A [35–38].

### *4.2. Dynamics and kinetics of force-dependent protein–protein interactions*

Magnetic tweezers not only can be applied to studies of the mechanical stability of proteins, but also can be utilized to understand force-dependent protein–protein interactions which play key roles in various mechanosensing processes [1,2]. This was demonstrated in recent studies of the force-dependent binding of the vinculin to talin and α-catenin [39,32,33], which are crucial in regulating the strength of cell-ECM focal adhesion and cell–cell adherens junctions, respectively [40–42].

These studies revealed that 5–10 pN forces are able to change the conformations of the talin rod domains and α-catenin modulation domains, exposing the cryptic vinculin sites buried in the folded conformations. This activates binding of vinculin to talin and α-catenin, with a dramatically increased binding affinity by more than 1000 folds. Further, it was demonstrated by these studies that the bound vinculin is displaced at high forces (>30 pN), resulting in an interesting biphasic force-dependence of vinculin binding. These results provide explanation of the mechanism by which talin and α-catenin can act as switches for mechanosensitive cellular signaling. There are many other mechanosensing proteins, such as focal adhesion kinase, α-actinin, cadherins, and β-catenin, acting as highly sensitive mechanical switches controlled by the physiological level of forces applied to them [1,2,42]. Therefore, similar studies using magnetic tweezers can be applied to understand their mechanosensing mechanisms, as sketched in Fig. 3.

## 5. Discussion

We have reviewed the working principles of magnetic tweezers, a theoretical framework to understand force-dependent stability

and interactions of mechanosensing proteins, and the recent applications in studies of mechanosensing proteins involved in regulations of muscle elasticity, focal adhesion, and cell–cell adherens junction, under physiological range of force. These recent studies show that magnetic tweezers, compared to other single-molecule manipulation techniques, excel in ultra-stable, long-time (over hours with negligible drift) measurements for complex reactions.

Most of the current magnetic tweezers are restricted to >1 nm spatial resolution and >1 ms temporal resolutions with bright-field illumination using beads with diameter of a few μm, which cannot be applied to study processes involving faster dynamics or smaller conformational changes. It is possible to significantly increase both spatial and temporal resolutions by using different height determination methods and using smaller beads. As demonstrated in a recent paper, a single gold nano particle of a diameter of ~100 nm can be visualized using dark-field TIRF microscopy [43]. In this method, the gold particle is illuminated by a thin layer (~200 nm) of the evanescent light wave, whose intensity exponentially decays with the height above the surface. Therefore, the height of the bead can be directly obtained by the intensity of the scattered light, without need for complex bead image analysis which is computationally costly. Another limitation of most current magnetic tweezers is the lack of the capability of direct 'visualization' of protein–protein interactions, which can be overcome by combination with fluorescence-based techniques as demonstrated in [16,17]. In addition, magnetic tweezers suffer from flow-perturbation during rapid solution exchange processes, which has been recently overcome by performing the experiments at the bottom of microholes in thin membranes [44].

Due to their unique strengths in studies of force-dependent structural stability and interactions, magnetic tweezers will have a wide scope of applications in mechanobiology, a current frontier of biology. In this emerging field, force has been recognized as a crucial determinant involved in various critical cellular processes such as cell differentiation, cell migration, tissue formation and repair [1,2]. Force plays its role through its effects on a set of force-bearing proteins, affecting their structural stability and interaction with other cellular factors. Therefore, studies of these proteins using magnetic tweezers will provide crucial insights into the mechanisms of various mechanosensing dependent cellular pathways, many of which are related to diseases such as cancer [1,2].

## Conflict of interest statement

None declared.

## Acknowledgements

We are grateful to Hu Chen (Xiamen University, China) and Mingxi Yao (Mechanobiology Institute, Singapore) for their discussions and proofreading of the manuscript. This work is supported by National Research Foundation of Singapore through the Mechanobiology Institute at National University of Singapore to J.Y.; Singapore Ministry of Education Academic Research Fund Tier 3 (MOE2012-T3-1-001) and Tier 2 (MOE2013-T2-1-154) to J.Y.

## References

[1] V. Vogel, M. Sheetz, Local force and geometry sensing regulate cell functions, Nat. Rev. Mol. Cell Biol. 7 (4) (2006) 265–275, http://dx.doi.org/10.1038/nrm1890.
[2] T. Iskratsch, H. Wolfenson, M.P. Sheetz, Appreciating force and shape—the rise of mechanotransduction in cell biology, Nat. Rev. Mol. Cell Biol. 15 (12) (2014) 825–833, http://dx.doi.org/10.1038/nrm3903.
[3] K.C. Neuman, A. Nagy, Single-molecule force spectroscopy: optical tweezers, magnetic tweezers and atomic force microscopy, Nat. Methods 5 (6) (2008) 491–505, http://dx.doi.org/10.1038/nmeth.1218.
[4] C. Grashoff, B.D. Hoffman, M.D. Brenner, R. Zhou, M. Parsons, M.T. Yang, M.A. McLean, S.G. Sligar, C.S. Chen, T. Ha, M.A. Schwartz, Measuring mechanical tension across vinculin reveals regulation of focal adhesion dynamics, Nature 466 (7303) (2010) 263–266. <http://dx.doi.org/10.1038/nature09198>.
[5] D.R. Stabley, C. Jurchenko, S.S. Marshall, K.S. Salaita, Visualizing mechanical tension across membrane receptors with a fluorescent sensor, Nat. Methods 9 (1) (2012) 64–67. <http://dx.doi.org/10.1038/nmeth.1747>.
[6] H. Chen, G. Yuan, R.S. Winardhi, M. Yao, I. Popa, J.M. Fernandez, J. Yan, Dynamics of equilibrium folding and unfolding transitions of titin immunoglobulin domain under constant forces, J. Am. Chem. Soc. 137 (10) (2015) 3540–3546, http://dx.doi.org/10.1021/ja5119368.
[7] T.R. Strick, J.F. Allemand, D. Bensimon, V. Croquette, Behavior of supercoiled dna, Biophys. J. 74 (4) (1998) 2016–2028, http://dx.doi.org/10.1016/S0006-3495(98)77908-1.
[8] J. Yan, D. Skoko, J.F. Marko, Near-field-magnetic-tweezer manipulation of single dna molecules, Phys. Rev. E 70 (2004) 011905.
[9] I. De Vlaminck, C. Dekker, Recent advances in magnetic tweezers, Annu. Rev. Biophys. 41 (2012) 453–472, http://dx.doi.org/10.1146/annurev-biophys-122311-100544.
[10] I. De Vlaminck, T. Henighan, M.T.J. van Loenhout, D.R. Burnham, C. Dekker, Magnetic forces and dna mechanics in multiplexed magnetic tweezers, PLoS One 7 (8) (2012) e41432, http://dx.doi.org/10.1371/journal.pone.0041432.
[11] H. Chen, H. Fu, X. Zhu, P. Cong, F. Nakamura, J. Yan, Improved high-force magnetic tweezers for stretching and refolding of proteins and short dna, Biophys. J. 100 (2) (2011) 517–523, http://dx.doi.org/10.1016/j.bpj.2010.12.3700.
[12] S. Le, H. Chen, P. Cong, J. Lin, P. Dröge, J. Yan, Mechanosensing of dna bending in a single specific protein-dna complex, Sci. Rep. 3 (2013) 3508, http://dx.doi.org/10.1038/srep03508.
[13] S. Le, H. Chen, X. Zhang, J. Chen, K.N. Patil, K. Muniyappa, J. Yan, Mechanical force antagonizes the inhibitory effects of recx on reca filament formation in mycobacterium tuberculosis, Nucl. Acids Res. 42 (19) (2014) 11992–11999, http://dx.doi.org/10.1093/nar/gku899.
[14] H. Fu, S. Le, H. Chen, K. Muniyappa, J. Yan, Force and atp hydrolysis dependent regulation of reca nucleoprotein filament by single-stranded dna binding protein, Nucl. Acids Res. 41 (2) (2013) 924–932, http://dx.doi.org/10.1093/nar/gks1162.
[15] R. Liu, S. Garcia-Manyes, A. Sarkar, C.L. Badilla, J.M. Fernández, Mechanical characterization of protein l in the low-force regime by electromagnetic tweezers/evanescent nanometry, Biophys. J. 96 (9) (2009) 3810–3821, http://dx.doi.org/10.1016/j.bpj.2009.01.043.
[16] M. Lee, S.H. Kim, S.-C. Hong, Minute negative superhelicity is sufficient to induce the b-z transition in the presence of low tension, Proc. Natl. Acad. Sci. USA 107 (11) (2010) 4985–4990, http://dx.doi.org/10.1073/pnas.0911528107.
[17] X. Long, J.W. Parks, C.R. Bagshaw, M.D. Stone, Mechanical unfolding of human telomere g-quadruplex dna probed by integrated fluorescence and magnetic tweezers spectroscopy, Biophys. J. 106 (2) (2013) 64a, http://dx.doi.org/10.1016/j.bpj.2013.11.430.
[18] Y. Qu, C.J. Lim, Y.R. Whang, J. Liu, J. Yan, Mechanism of dna organization by mycobacterium tuberculosis protein lsr2, Nucl. Acids Res. 41 (10) (2013) 5263–5272, http://dx.doi.org/10.1093/nar/gkt249.
[19] J. Lin, H. Chen, P. Dröge, J. Yan, Physical organization of dna by multiple non-specific dna-binding modes of integration host factor (ihf), PLoS One 7 (11) (2012) e49885, http://dx.doi.org/10.1371/journal.pone.0049885.
[20] J.S. Graham, R.C. Johnson, J.F. Marko, Concentration-dependent exchange accelerates turnover of proteins bound to double-stranded dna, Nucl. Acids Res. 39 (6) (2011) 2249–2259, http://dx.doi.org/10.1093/nar/gkq1140.
[21] H. Fu, H. Chen, X. Zhang, Y. Qu, J.F. Marko, J. Yan, Transition dynamics and selection of the distinct s-dna and strand unpeeling modes of double helix overstretching, Nucl. Acids Res. 39 (8) (2011) 3473–3481, http://dx.doi.org/10.1093/nar/gkq1278.
[22] X. Zhang, H. Chen, H. Fu, P.S. Doyle, J. Yan, Two distinct overstretched dna structures revealed by single-molecule thermodynamics measurements, Proc. Natl. Acad. Sci. USA 109 (21) (2012) 8103–8108, http://dx.doi.org/10.1073/pnas.1109824109.
[23] X. Zhang, H. Chen, S. Le, I. Rouzina, P.S. Doyle, J. Yan, Revealing the competition between peeled ssdna, melting bubbles, and s-dna during dna overstretching by single-molecule calorimetry, Proc. Natl. Acad. Sci. USA 110 (10) (2013) 3865–3870, http://dx.doi.org/10.1073/pnas.1213740110.
[24] H. You, X. Zeng, Y. Xu, C.J. Lim, A.K. Efremov, A.T. Phan, J. Yan, Dynamics and stability of polymorphic human telomeric g-quadruplex under tension, Nucl. Acids Res. 42 (13) (2014) 8789–8795, http://dx.doi.org/10.1093/nar/gku581.
[25] H. You, J. Wu, F. Shao, J. Yan, Stability and kinetics of c-myc promoter g-quadruplexes studied by single-molecule manipulation, J. Am. Chem. Soc. 137 (7) (2015) 2424–2427, http://dx.doi.org/10.1021/ja511680u.
[26] M. Yao, H. Chen, J. Yan, Thermodynamics of force-dependent folding and unfolding of small protein and nucleic acid structures, Integr. Biol. (2015), http://dx.doi.org/10.1039/c5ib00038f.
[27] C. Bustamante, J.F. Marko, E.D. Siggia, S. Smith, Entropic elasticity of lambda-phage dna, Science 265 (5178) (1994) 1599–1600.
[28] J.F. Marko, E.D. Siggia, Stretching dna, Macromolecules 28 (26) (1995) 8759–8770, http://dx.doi.org/10.1021/ma00130a008.
[29] I. Rouzina, V.A. Bloomfield, Force-induced melting of the dna double helix 1. Thermodynamic analysis, Biophys. J. 80 (2) (2001) 882–893, http://dx.doi.org/10.1016/S0006-3495(01)76067-5.
[30] S. Cocco, J. Yan, J.-F. Léger, D. Chatenay, J.F. Marko, Overstretching and force-driven strand separation of double-helix dna, Phys. Rev. E 70 (2004) 011910.

[31] Y. Gao, S. Zorman, G. Gundersen, Z. Xi, L. Ma, G. Sirinakis, J.E. Rothman, Y. Zhang, Single reconstituted neuronal snare complexes zipper in three distinct stages, Science 337 (6100) (2012) 1340–1343, http://dx.doi.org/10.1126/science.1224492. <http://www.ncbi.nlm.nih.gov/pmc/articles/PMC3677750/>.
[32] M. Yao, W. Qiu, R. Liu, A.K. Efremov, P. Cong, R. Seddiki, M. Payre, C.T. Lim, B. Ladoux, R.-M. Mège, J. Yan, Force-dependent conformational switch of α-catenin controls vinculin binding, Nat. Commun. 5 (2014) 4525, http://dx.doi.org/10.1038/ncomms5525.
[33] M. Yao, B.T. Goult, H. Chen, P. Cong, M.P. Sheetz, J. Yan, Mechanical activation of vinculin binding to talin locks talin in an unfolded conformation, Sci. Rep. 4 (2014) 4610, http://dx.doi.org/10.1038/srep04610.
[34] J. Trinick, Cytoskeleton: titin as a scaffold and spring, Curr. Biol. 6 (3) (1996) 258–260, http://dx.doi.org/10.1016/S0960-9822(02)00472-4.
[35] J.M. Fernandez, H. Li, Force-clamp spectroscopy monitors the folding trajectory of a single protein, Science 303 (5664) (2004) 1674–1678, http://dx.doi.org/10.1126/science.1092497.
[36] L. Rognoni, J. Stigler, B. Pelz, J. Ylänne, M. Rief, Dynamic force sensing of filamin revealed in single-molecule experiments, Proc. Natl. Acad. Sci. USA 109 (48) (2012) 19679–19684, http://dx.doi.org/10.1073/pnas.1211274109.
[37] H. Chen, X. Zhu, P. Cong, M.P. Sheetz, F. Nakamura, J. Yan, Differential mechanical stability of filamin a rod segments, Biophys. J. 101 (5) (2011) 1231–1237, http://dx.doi.org/10.1016/j.bpj.2011.07.028.
[38] H. Chen, S. Chandrasekar, M.P. Sheetz, T.P. Stossel, F. Nakamura, J. Yan, Mechanical perturbation of filamin a immunoglobulin repeats 20–21 reveals potential non-equilibrium mechanochemical partner binding function, Sci. Rep. 3 (2013) 1642, http://dx.doi.org/10.1038/srep01642.
[39] A. del Rio, R. Perez-Jimenez, R. Liu, P. Roca-Cusachs, J.M. Fernandez, M.P. Sheetz, Stretching single talin rod molecules activates vinculin binding, Science 323 (5914) (2009) 638–641, http://dx.doi.org/10.1126/science.1162912.
[40] S. Yonemura, Y. Wada, T. Watanabe, A. Nagafuchi, M. Shibata, [alpha]-catenin as a tension transducer that induces adherens junction development, Nat. Cell Biol. 12 (6) (2010) 533–542.
[41] J. Yan, M. Yao, B. Goult, M. Sheetz, Talin dependent mechanosensitivity of cell focal adhesions, Cell Mol. Bioeng. 8 (1) (2015) 151–159, http://dx.doi.org/10.1007/s12195-014-0364-5.
[42] X. Liang, G. Gomez, A. Yap, Current perspectives on cadherin-cytoskeleton interactions and dynamics, Cell Health Cytoskeleton 7 (2015) 11–24.
[43] P. Lebel, A. Basu, F.C. Oberstrass, E.M. Tretter, Z. Bryant, Gold rotor bead tracking for high-speed measurements of dna twist, torque and extension, Nat. Methods 11 (4) (2014) 456–462, http://dx.doi.org/10.1038/nmeth.2854.
[44] S. Le, M. Yao, J. Chen, A.K. Efremov, S. Azimi, J. Yan, Disturbance-free rapid solution exchange for magnetic tweezers single-molecule studies, Nucl. Acids Res. (2015), http://dx.doi.org/10.1093/nar/gkv554.